1

Introduction to Circularly Polarized Antennas

1.1 Introduction

Circularly polarized (CP) antennas are a type of antenna with circular polarization. Due to the features of circular polarization, CP antennas have several important advantages compared to antennas using linear polarizations, and are becoming a key technology for various wireless systems including satellite communications, mobile communications, global navigation satellite systems (GNSS), wireless sensors, radio frequency identification (RFID), wireless power transmission, wireless local area networks (WLAN), wireless personal area networks (WPAN), Worldwide Interoperability for Microwave Access (WiMAX) and Direct Broadcasting Service (DBS) television reception systems. Lots of progress in research and development has been made during recent years.

The CP antenna is very effective in combating multi-path interferences or fading [1,2]. The reflected radio signal from the ground or other objects will result in a reversal of polarization, that is, right-hand circular polarization (RHCP) reflections show left-hand circular polarization (LHCP). A RHCP antenna will have a rejection of a reflected signal which is LHCP, thus reducing the multi-path interferences from the reflected signals.

The second advantage is that CP antenna is able to reduce the 'Faraday rotation' effect due to the ionosphere [3,4]. The Faraday rotation effect causes a significant signal loss (about 3 dB or more) if linearly polarized signals are employed. The CP antenna is immune to this problem, thus the CP antenna is widely used for space telemetry applications of satellites, space probes and ballistic missiles to transmit or receive signals that have undergone Faraday rotation by travelling through the ionosphere.

Another advantage of using CP antennas is that no strict orientation between transmitting and receiving antennas is required. This is different from linearly polarized antennas which are subject to polarization mismatch losses if arbitrary polarization misalignment occurs between transmitting and receiving antennas. This is useful for mobile satellite communications where it is difficult to maintain a constant antenna orientation. With CP, the strength of the received signals is fairly constant regardless of the antenna orientation. These advantages make CP antennas very attractive for many wireless systems.

Circularly Polarized Antennas, First Edition. Steven (Shichang) Gao, Qi Luo and Fuguo Zhu.

This chapter serves as a basis for the chapters that follow. It will introduce some basic parameters of antennas. Different types of basic CP antennas such as CP microstrip patch antenna, helix, quadrifilar helix antenna (QHA), printed quadrifilar helix antenna (PQHA), spiral antenna, CP dielectric resonator antenna (DRA), CP slot antennas, CP horns and CP arrays will be described and basic designs illustrated. Typical requirements and challenges in CP antenna designs will be discussed at the end.

1.2 Antenna Parameters

An antenna is a device which can receive or/and transmit radio signals. As a receiving device, it can collect the radio signals from free space and convert them from electromagnetic waves (in the free space) into guided waves in transmission lines; as a transmitting device, it can transmit radio signals to free space by converting the guided waves in transmission lines into the electromagnetic waves in the free space. In some cases, an antenna can serve both functions of receive and transmit.

Figure 1.1 depicts the basic operation of a transmit antenna. As shown, the information (voice, image or data) is processed in a radio transmitter and then the output signal from the transmitter propagates along the transmission lines before finally being radiated by the antenna. The antenna converts the guided-wave signals in the transmission lines into electromagnetic waves in the free space. The operation of a receive antenna follows a reverse process, that is, collecting the radio signals by converting the electromagnetic waves in free space into guided-wave signals in the transmission lines, which are then fed into radio receivers.

1.2.1 Input Impedance

The input impedance Z_{in} is defined as the impedance presented by an antenna at its feed point, or the ratio of the voltage to current at the feed point [5]. The input impedance is usually a complex number which is also frequency dependent. It can be expressed as

$$Z_{in} = R_{in} + jX_{in} \tag{1.1}$$

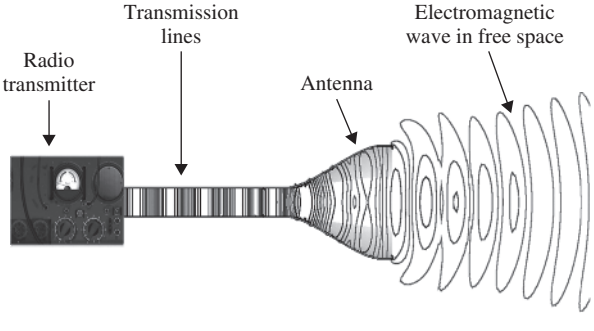

Figure 1.1 Basic operations of a transmit antenna

The real part of the impedance, R_{in}, includes the radiation resistance R_r of the antenna and the loss resistance R_L. R_r relates to the power radiated by the antenna, and R_L relates to the power dissipated in the antenna due to losses in dielectric materials, antenna conductor losses, and so on.

1.2.2 Reflection Coefficient, Return Loss and Voltage Standing Wave Ratio

The antenna input impedance needs to be matched with the characteristic impedance of the transmission line connected to the feed point of the antenna. Usually a 50 Ω cable is used to feed the antenna. Thus the antenna input impedance needs to be equal to 50 Ω, otherwise there will be an impedance mismatch at the antenna feed point. In the case of impedance mismatch, there will be signal reflections, that is, some of signals fed to the antenna will be reflected back to the signal sources.

The reflection coefficient Γ denotes the ratio of the reflected wave voltage to the incident wave voltage [5]. The reflection coefficient at the feed point of the antenna can be related to the antenna input impedance by the following equation:

$$\Gamma = \frac{Z_{in} - Z_0}{Z_{in} + Z_0} \tag{1.2}$$

Here, Z_{in} and Z_o denote the input impedance of the antenna, and the characteristic impedance of the transmission line connected to the antenna feed point, respectively. As shown in equation (1.2), the reflection coefficient is zero if Z_{in} is equal to Z_o.

Return loss (in dB) is defined as:

$$RL = -20 \log |\Gamma|$$

For a well-designed antenna, the required return loss should usually be at least 10 dB, though some antennas on small mobile terminals can only achieve about 6 dB. Voltage Standing Wave Ratio (VSWR) is the ratio of the maximum voltage $V_{\max}$ to the minimum voltage $V_{\min}$ on the transmission line. It is defined as:

$$VSWR = \frac{|V_{\max}|}{|V_{\min}|} = \frac{1 + |\Gamma|}{1 - |\Gamma|} \tag{1.3}$$

1.2.3 Radiation Patterns

The radiation pattern of the antenna illustrates the distribution of radiated power in the space [6–9]. It can be plotted in a spherical coordinate system as the radiated power versus the elevation angle (θ) or the azimuth angle (φ). Figure 1.2 shows a radiation pattern plotted as the radiated power versus the elevation angle (θ). As shown, the radiation pattern has a few lobes. The main lobe is the lobe containing the majority of radiated power. The lobe radiating towards the backward direction is the back lobe. Usually there will also be a few other small lobes called the side lobes. The 3-dB beamwidth indicated in the figure refers to the angular range between two points where the radiated power is half the maximum radiated power. Figure 1.2 shows the radiation pattern in the elevation plane. There is also

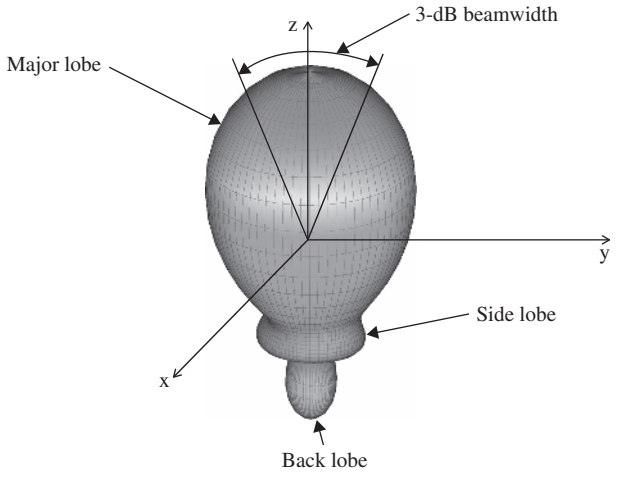

Figure 1.2 A directional radiation pattern in the elevation plane

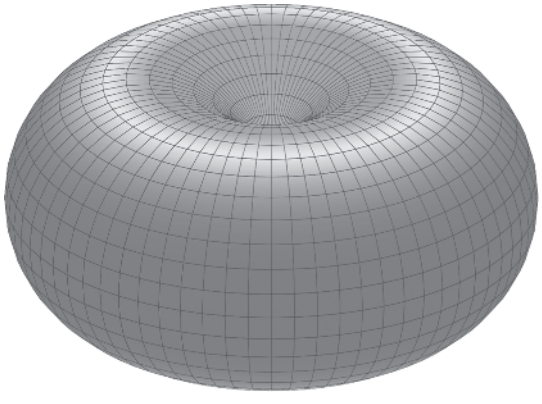

Figure 1.3 Omni-directional pattern

the radiation pattern in the azimuth plane, which can be plotted as the radiated power versus the azimuth angle (φ). The antenna pattern can be isotropic, directional or omni-directional. An isotropic pattern is uniform in all directions, which does not exist in reality. The pattern in Figure 1.2 is directional. As shown in Figure 1.2, the majority of radiated power is focused at one direction and the maximum radiation is along the z axis. An omni-directional pattern is donut-shaped, as shown in Figure 1.3.

1.2.4 Directivity, Gain and Efficiency

A practical antenna usually radiates in certain directions. The directivity, $D(\theta, \varphi)$, is defined as the radiated power per unit solid angle compared to what would be received by an isotropic

radiator [6–9]. It can be calculated by

$$D(\theta, \varphi) = \frac{r^2 \cdot \frac{1}{2}\mathrm{Re}[E \times H^*]}{P_{rad}/4\pi} = \frac{2\pi r^2 \cdot \mathrm{Re}[E \times H^*]}{P_{rad}} \tag{1.4}$$

where E, H, r and P_{rad} denote the peak value of electric field, the peak value of magnetic field, the distance between the source and test point, and the radiated power from the antenna, respectively. It is also assumed that the test point is in the far field region of the antenna, which means the distance $r > \frac{2D^2}{\lambda}$ [6–9]. Here D is the maximum dimension of the antenna and λ is the wavelength.

The gain of the antenna is similar as the directivity though it includes the efficiency η of the antenna, since some power will be lost in the antenna.

$$G(\theta, \varphi) = \eta \cdot D(\theta, \varphi) \tag{1.5}$$

Both directivity and gain are normally expressed in dB. It is common practice to write the antenna gain in dBi, which means that it is defined relative to an isotropic radiator.

1.2.5 Linear Polarization, Circular Polarization and Axial Ratio

Polarization of an antenna is related to the orientations of electric fields radiated by the antenna. Assuming a half-wavelength dipole is vertically oriented above the Earth, it will produce radiated fields in the far field and the radiated electric fields will be dominated by $E_\theta(\theta, \varphi)$. In this case, the polarization of the dipole is called *vertical polarization*. On the other hand, if a half-wavelength dipole is horizontally oriented above the Earth, the radiated electric fields of the antenna will be dominated by $E_\varphi(\theta, \varphi)$ in the far field. The polarization of the antenna is then called *horizontal polarization*. Both vertical and horizontal polarizations are *linear polarizations*. Linearly polarized antennas are commonly used in terrestrial wireless communications.

To produce circular polarization, two orthogonal components of electric fields in the far field region are required [6–10]. The electrical field radiated by an antenna can be written as

$$\vec{E}(\theta, \varphi) = \vec{\theta} E_\theta(\theta, \varphi) e^{j\phi_1} + \vec{\varphi} E_\varphi(\theta, \varphi) e^{j\phi_2} \tag{1.6}$$

Here $E_\theta(\theta, \varphi)$ and $E_\varphi(\theta, \varphi)$ denote the magnitudes of electric field components in the far field of the antenna. ϕ_1 and ϕ_2 denote the phase shift of each field component.

Circular polarization can be achieved only if the total electric field has two orthogonal components which have the same magnitudes and a 90° phase difference between the two components. That is

$$\begin{aligned} E_\theta(\theta, \varphi) &= E_\varphi(\theta, \varphi) \\ \phi_2 - \phi_1 &= \pm\frac{\pi}{2} \end{aligned} \tag{1.7}$$

For a circularly polarized wave, the electric field vector at a given point in space traced as a function of time is a circle. The sense of rotation can be determined by observing the direction of the field's temporal rotation as the wave is viewed along the direction of wave

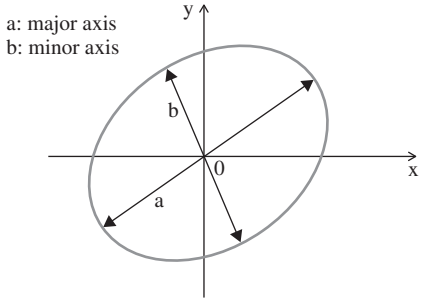

Figure 1.4 Polarization ellipse traced at a certain position as a function of time

propagation: if the field rotation is clockwise, the wave is RHCP; if the field rotation is anti-clockwise, the wave is LHCP.

In reality, it is impossible to achieve a perfect circular polarization, thus the curve traced at a given position as a function of time is usually an ellipse, as shown in Figure 1.4. Lines a and b denote the major axis and the minor axis of polarization ellipse, respectively. The ratio of the major axis to the minor axis of the ellipse is termed as the axial ratio (AR) [6–10].

$$AR = \frac{a}{b} \tag{1.8}$$

AR is a key parameter for measuring the circular polarization. Usually AR is required to be below 3 dB for a CP antenna.

1.2.6 Bandwidth and Resonant Frequency

Usually an antenna is designed to operate within a specified frequency range. The bandwidth of an antenna is usually determined by the frequency range within which the key parameter of the antenna satisfies a certain requirement, for example, minimum return loss of 10 dB. At the resonant frequency of an antenna, the antenna input impedance is purely resistive. Often the resonant frequency is chosen as the centre of the frequency bandwidth of an antenna. The bandwidth of an antenna can be calculated by using the upper and lower edges of the achieved frequency range:

$$BW = \frac{f_2 - f_1}{f_o} \times 100\% \tag{1.9}$$

where f_1 is the lower edge of the achieved frequency range,

f_2 is the upper edge of the achieved frequency range, and
f_o is the centre frequency of the range.

Note that this definition is for antennas with a bandwidth below 100%. For antenna bandwidths over 100%, the bandwidth can be calculated using the ratio between the upper and lower edge of frequencies. For a linearly polarized antenna, the input impedance is usually the most sensitive parameter compared to other antenna parameters such as radiation patterns, gain and polarization. Thus the bandwidth of a linearly polarized antenna is often

referred to as the 'impedance bandwidth', but it can also be to do with other parameters such as radiation patterns, gain and polarization.

When evaluating the bandwidth of CP antennas, one must check both the impedance bandwidth and the bandwidth of AR, that is, the frequency range within which the AR is below 3 dB. A good impedance matching does not necessarily lead to a good gain or a low AR value. The impedance bandwidth of an antenna can be broadened using suitable impedance matching networks, while the AR bandwidth can be broadened by using a broadband phase shifter network [5].

1.3 Basic CP Antenna Types

1.3.1 CP Microstrip Patch Antennas

Microstrip patch antenna is one very popular type of antennas, due to its advantages of low profile, easy fabrication, low cost and conformability to curved surfaces. Circular polarization in patch antennas can be achieved using a multi-feed technique or a single-feed technique [6–9,11–13].

Figure 1.5 shows a simple CP microstrip patch antenna using a dual-feed technique. Both the top and side views of the antenna are shown in Figure 1.5. To produce circular polarization, a square microstrip patch is fed by two orthogonal microstrip feedlines as shown in Figure 1.5(a). Two microstrip feed lines excite the patch antenna in TM_{01} and TM_{10} modes so that it radiates both a horizontally polarized wave and a vertically polarized wave simultaneously [6–9,11–13]. A microstrip hybrid is employed in Figure 1.5(a) to produce a 90° phase difference between two orthogonally polarized waves. Figure 1.5(b) shows the side view of the antenna. The metallic patch is etched on the top of a dielectric substrate having thickness h and relative permittivity ε_r. The dielectric substrate is backed by a metallic ground plane. To design the antenna resonant at a frequency f_o, the length L of the patch can be approximately calculated by using the following equation:

$$L \approx \frac{c}{2f_o\sqrt{\dfrac{\varepsilon_r + 1}{2}}} \tag{1.10}$$

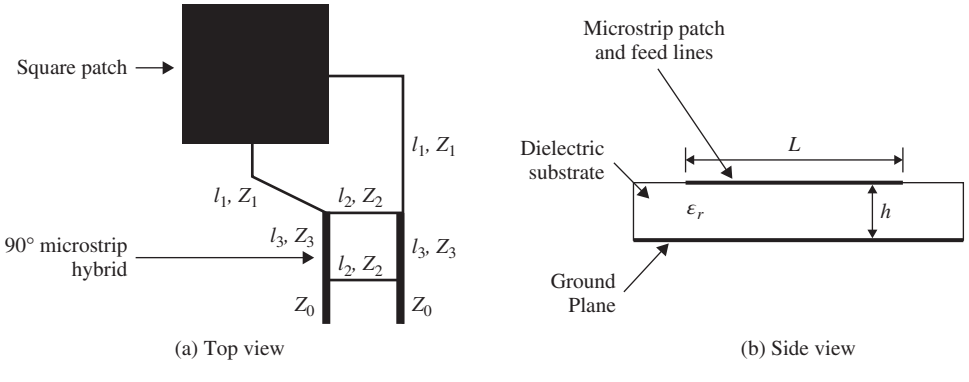

Figure 1.5 A microstrip line-feed patch antenna with a 90° hybrid

where c is the velocity of light. To achieve accurate antenna designs, full-wave electromagnetic simulators can be employed to do simulations and optimizations of the dimensions of antenna. The results from equation (1.10) can be used as an initial value for the antenna optimization.

As shown in Figure 1.5(a), two microstrip feed lines connect the square patch and two ports of the microstrip 90° hybrid. The microstrip line serves as an impedance transformer between the input of the antenna and the input ports of the hybrid. The length (l_1) and characteristic impedance (Z_1) of the microstrip feed lines can be calculated by

$$\begin{aligned} l_1 &= \frac{\lambda_g}{4} \\ Z_1 &= \sqrt{Z_{in} Z_0} \end{aligned} \tag{1.11}$$

where λ_g is the guided wavelength of the microstrip line,

Z_{in} is the input impedance of the patch antenna, and
Z_0 is the characteristic impedance of the microstrip line at the input of hybrid circuit.

The microstrip 90° hybrid circuit consists of four sections of microstrip lines. The following equations can be employed to determine the length and width of each section of microstrip lines:

$$\begin{aligned} l_2 = l_3 &= \frac{\lambda_g}{4} \\ Z_2 &= Z_0 \\ Z_3 &= \frac{Z_0}{\sqrt{2}} \end{aligned} \tag{1.12}$$

where l_2 and l_3 denote the length of microstrip lines as indicated in Figure 1.5(a), Z_2 and Z_3 denote the characteristic impedance of microstrip line sections indicated in Figure 1.5(a).

The characteristic impedance of the microstrip line at the input of hybrid circuit, Z_0, is usually chosen to be 50 Ω. The microstrip hybrid circuit is easy to be fabricated and has been widely used in CP antennas. One drawback of microstrip hybrid circuit is the large size. Many techniques have been developed to reduce the size of microstrip hybrid, for example, by using 'Π network' with stub loading or lumped-element loading of transmission lines [5,14,15]. The hybrid circuit can also be implemented by using lumped elements or left-handed transmission lines [14,15].

The CP patch antenna can also use other feeding structures, such as probe feeds, slot-coupled feeds, electromagnetically-coupled feed and coplanar waveguide (CPW) feeds. Figures 1.6 and 1.7 show a CP patch antenna using two probe feeds, and a CP patch with slot-coupled feeds, respectively. Both the top view and side view of the antenna are shown in Figure 1.6. As shown, circular polarization is obtained by feeding a square patch with a 90° phase difference between two feed probes placed symmetrically on the two orthogonal edges of the patch. In this case, an external phase shifter is required for producing the 90° phase difference between two feeds. The antenna in Figure 1.7 employs a microstrip hybrid circuit for producing the 90° phase difference between two feeds. The microstrip hybrid is put at the bottom of the antenna, and coupled to the square patch on the top via

Figure 1.6 A probe-feed patch antenna with an external 90° phase shifter

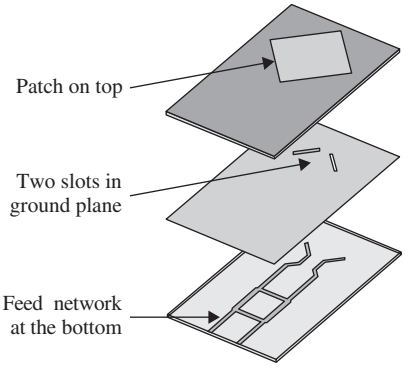

Figure 1.7 Slot-coupled CP patch antenna (dual feed with a hybrid coupler)

two orthogonal slots cut in the ground plane. The slot-coupled CP antenna has been widely used in wireless systems during recent years, as it has many advantages compared to CP antennas using other feed structures: (1) It allows the patch antenna and the feed circuits to employ different dielectric substrate so that both the patch antenna and the feed circuits can achieve optimized performance; (2) It is easy to integrate active circuits with the feed network; (3) The parasitic radiation of feed network is reduced due to the isolation of the ground plane. The slot-coupled CP patch antenna is a popular choice for radiating elements in phased arrays for satellite communications.

For the dual-feed antenna, the radiating patch can use different shapes, such as square, circular, annular ring, and so on. Figure 1.8 shows a circular patch integrated with a microstrip hybrid circuit. As shown, the antenna can achieve either RHCP or LHCP, depending on the choice of input port.

To design the CP antenna in Figure 1.8, an approximate solution to the radius of patch is given by [6,7]:

$$a \approx \frac{F}{\sqrt{1+\dfrac{200h}{\pi\varepsilon_r F}\left[In\left(\dfrac{\beta F}{200h}\right)+1.7726\right]}}$$

$$F = \frac{8.791\times 10^9}{f_o\sqrt{\varepsilon_r}} \tag{1.13}$$

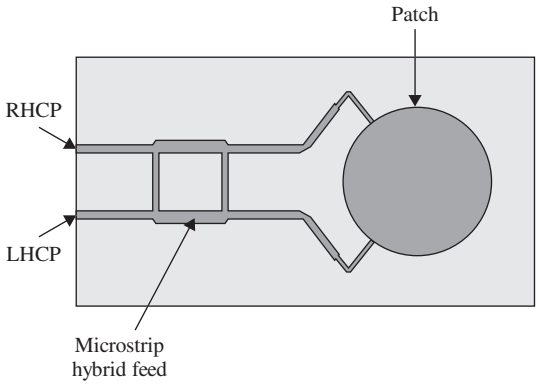

Figure 1.8 Circular patch integrated with a hybrid coupler

where a is the radius of circular patch,

f_o is the resonant frequency of the CP antenna in TM_{11} mode
ε_r is the relative permittivity of the dielectric substrate, and
h is the thickness of the substrate.

Besides the use of two feeds, it is also possible to excite circular polarization using more than two feeds. For example, circular polarization in the patch antenna can be excited using four feeds orthogonally located at four edges of a square patch and with an appropriate phase difference. Such a multi-feed technique can suppress higher order modes, and provide high polarization purity and a broad bandwidth at the expense of large size and complexity of feed network [13].

To simplify the feed network of CP patch antennas, a single-feed technique has been developed. Figure 1.9 shows six different configurations of single-feed CP microstrip patch antennas [12,13]. Such a technique requires the perturbation of the patch shape. For example, Figure 1.9(a) shows an elliptical patch fed along a line 45° from its major axis. The elliptical patch can be regarded as a circular patch with perturbations. The perturbation of the patch shape is used to excite two orthogonal modes with a $\pm 90^o$ phase difference. To design the CP antenna using a single-feed elliptical patch, the ratio between the major axis and minor axis is given by:

$$\frac{a}{b} = 1 + \frac{1.0887}{Q} \tag{1.14}$$

The value of antenna quality factor Q can be computed using the cavity model [6,7,12,13]. Alternatively, one can either measure the Q of the antenna experimentally, or use results from a full-wave electromagnetic analysis to estimate Q.

$$Q = \frac{f_o}{\Delta f} \frac{VSWR - 1}{\sqrt{VSWR}} \tag{1.15}$$

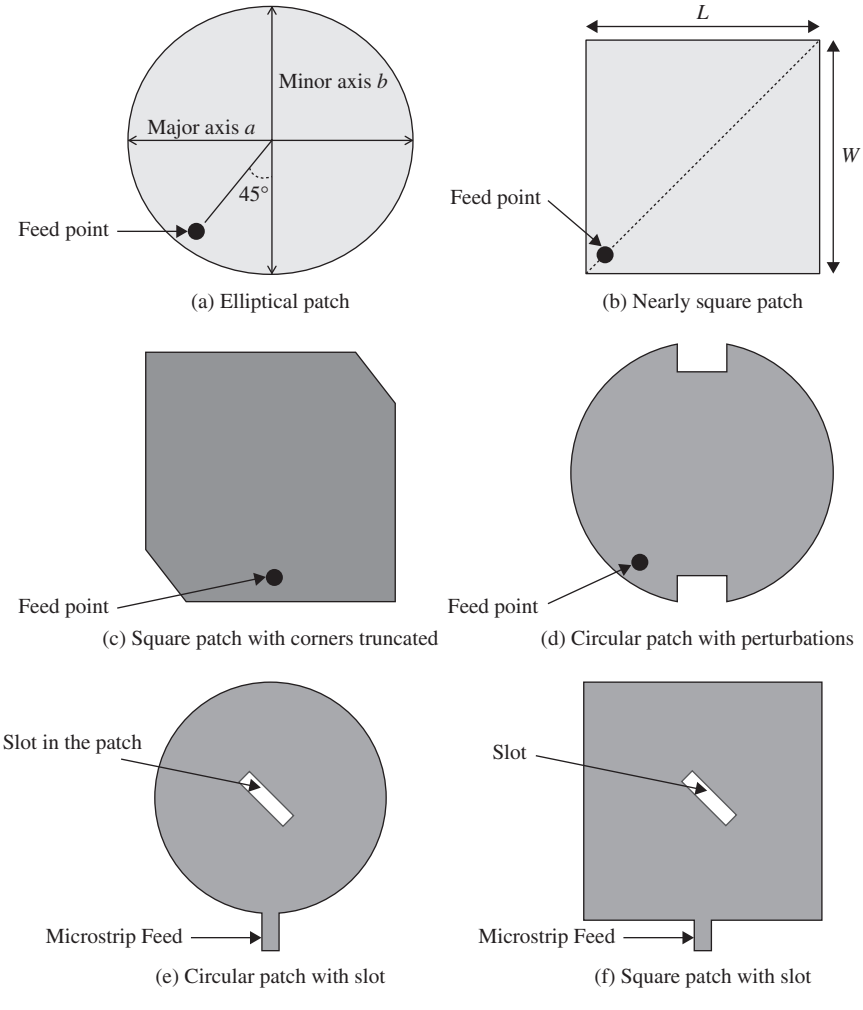

Figure 1.9 Single-feed CP patch antenna

where f_o is the resonant frequency of the antenna, and

Δf is the bandwidth of the antenna.

Another option for single-feed CP patch antenna design is to use the configuration shown in Figure 1.9(b), which is a nearly square patch fed at a point along the diagonal line of the patch. The length and width of the patch are L and W, respectively. The condition of circular polarization is satisfied when

$$L = W\left(1 + \frac{1}{Q}\right) \tag{1.16}$$

The value of antenna quality factor Q can be computed using equation (1.15). The resonant frequencies f_1 and f_2 associated with the length L and width W of a rectangular microstrip patch are

$$f_1 = \frac{f_o}{\sqrt{1+\frac{1}{Q}}}$$
$$f_2 = f_o\sqrt{1+\frac{1}{Q}} \tag{1.17}$$

where f_o is the centre frequency of the bandwidth.

Figure 1.9(c) and (d) show a square patch with two corners truncated, and a circular patch with two notches, respectively. Both antennas employ a single probe feed and the feed position is indicated in the figure. The perturbation can also take the form of a narrow slot cut in the centre of the patch, as shown in Figure 1.9(e) and (f). Other shapes of single-feed patch antennas, using pentagons, annual elliptic patches, and so on have also been reported [12,13]. The single-feed technique does not require a complicated feed network as in the multi-feed CP patch antennas, and is compact in size. The main drawback of this technique is the narrowband AR performance, typically 1–2%.

As in the case of multi-feed CP patch antenna, the single-feed CP antenna can also use different feed structures. Figure 1.10 shows a slot-coupled single-feed patch antenna. As shown, a circular patch with two notches is put on the top of dielectric substrate. The feed network is coupled to the patch via a single slot cut in the ground plane. Due to the use of a single slot, the feed network is much simpler compared to the dual-feed CP antenna in Figure 1.7. The slot can produce bi-directional radiation. To reduce the backward radiation from the slot, another ground plane can be added at the bottom, as shown in Figure 1.10. In this case, the feed network uses the stripline instead of microstrip lines, and usually vias are added between two ground planes for avoiding the excitation of parallel-plate modes in the stripline circuits [13].

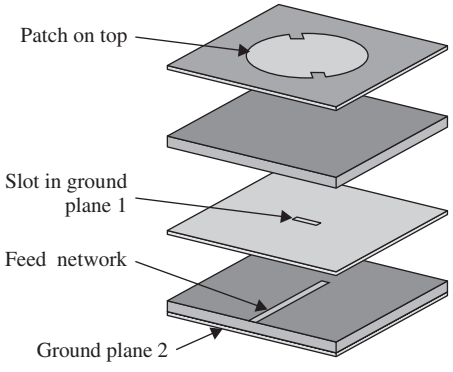

Figure 1.10 Slot-coupled single-feed patch antenna

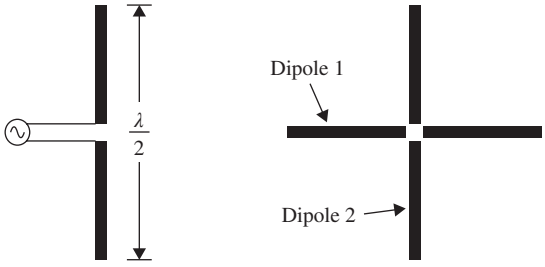

Figure 1.11 A dipole and a crossed dipole antenna

1.3.2 CP Wire Antennas

Crossed dipoles using wires have been employed to obtain circular polarization for many years. Figure 1.11 shows a dipole antenna and a crossed dipole antenna. The half-wavelength dipole in Figure 11(a) is vertically polarized and has an omni-directional pattern. For a crossed dipole in Figure 1.11(b), two dipoles are mounted perpendicular to each other and fed with a 90^o phase difference between them. The 90^o phase network can employ one quarter-wavelength of coaxial cable.

1.3.3 Helix Antennas

The helix antenna is one of the most promising antenna types for CP applications [6,9,11]. Figure 1.12 shows a helix antenna. It is basically a conducting wire wound in the form of a screw thread. Key design parameters of a helix antenna include the diameter of one turn (D), circumference of one turn (C), vertical separation between turns (S), the number of turns (N) and pitch angle (α), which controls how far the helix antenna grows in the axial-direction per turn.

The helix antenna has gained wide application because of its simple structure, wide operation bandwidth and circular polarization. The helix antenna can operate at three different modes [6,9,11]:

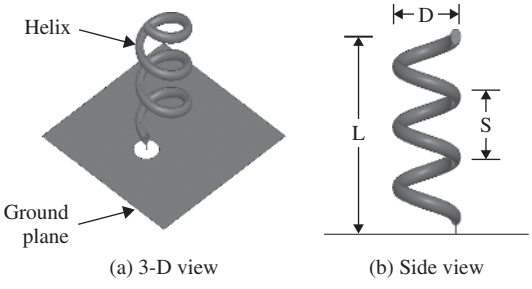

Figure 1.12 Helix antenna

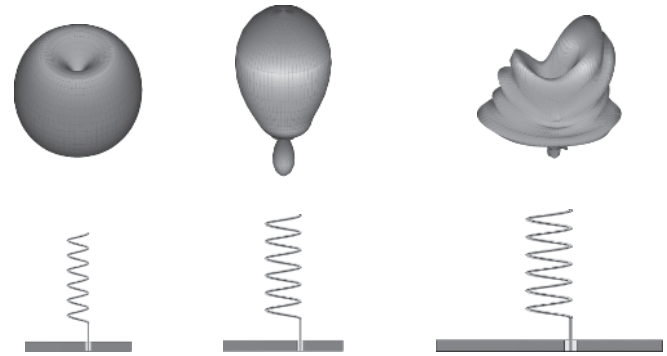

Figure 1.13 Axial, normal and higher order radiation modes of helix antenna [10,16]

- *Normal mode*, which occurs when the diameter of the helix is relatively small compared to the wavelength. The radiation pattern is omni-directional as shown in Figure 1.13(a).
- *Axial mode*, which occurs when the circumference of the helix is of the order of one wavelength. The maximum radiation is along the axis of the helix, as shown in Figure 1.13(b).
- *Higher-order radiation mode*, which occurs when the dimensions of the helix exceed those required for the axial mode. The major lobe is split-up as shown in Figure 1.13(c).

The axial mode is the one of major interests for CP applications. The normal-mode helix is useful for terminals in terrestrial cellular systems but not CP applications. The following gives the design equations for key design parameters of the helix so that it can achieve optimum performance in the axial mode [6,7,9]:

$$\begin{aligned} \frac{3}{4}\lambda < C < \frac{4}{3}\lambda \\ S \approx \frac{1}{4}\lambda \\ 12^0 \leq \alpha \leq 14^0 \end{aligned} \tag{1.18}$$

where λ is the free-space wavelength.

To understand how circular polarization is produced by a helix antenna, the helix can be approximated by N small loops and N short dipoles connected together in series. Two orthogonally polarized fields are produced by the loops and the dipoles, respectively. Here the planes of the loops are parallel to each other and perpendicular to the axes of the vertical dipoles. A 90^o phase difference between these two orthogonal fields is obtained if the vertical separation between turns S is chosen to be one quarter-wavelength as given in equation (1.18). The helix antenna has inherently broadband properties, possessing desirable radiation patterns, impedance and polarization characteristics over a relatively wide frequency range. The axial mode pattern exists for a nearly 2 to 1 frequency range because the natural adjustment of phase velocity results in the fields from the different turns adding in phase in the axial direction. The input impedance remains almost constant because of the large

attenuation to the reflected waves from the open end, and the antenna polarization remains circular because the in-phase field condition is a condition for circular polarization too [9].

1.3.4 Quadrifilar Helix Antennas and Printed Quadrifilar Helix Antennas

The QHA is one of the most commonly used antennas for satellite communications and Global Positioning Systems (GPS) applications [9,16–19]. The QHA can produce a cardioid-shaped radiation pattern with excellent circular polarization over a wide angular range. Such a pattern is suitable for GPS as it allows more satellites to be visible. Figure 1.14 shows two typical configurations of QHA antennas. Basically, a QHA consists of four identical helices interleaved with each other. Four identical helices are fed with a separate phase quadrature network which provides 0°, 90°, 180° and 270° phases to each of four helices, respectively. The helices can be shorted circuited or open-circuited at the end, as shown in Figure 1.14(a) and (b), respectively. QHA has important features of versatility and flexibility, due to the many degrees of freedom; such as the total length of each helical element, the number of turns, radius of helix, pitch angle, axial length and so on. In addition to the cardioid-shaped pattern, optimum choice of antenna parameters in QHA can lead to other types of radiation patterns, gain and bandwidth performance so that it can be used in a variety of applications for satellite communications and terrestrial systems. The QHA is a resonant radiating structure when the total length of each helical element, L_{total}, is equal to an integer number of quarter wavelengths [9].

$$L_{total} = N\frac{\lambda}{4} \tag{1.19}$$

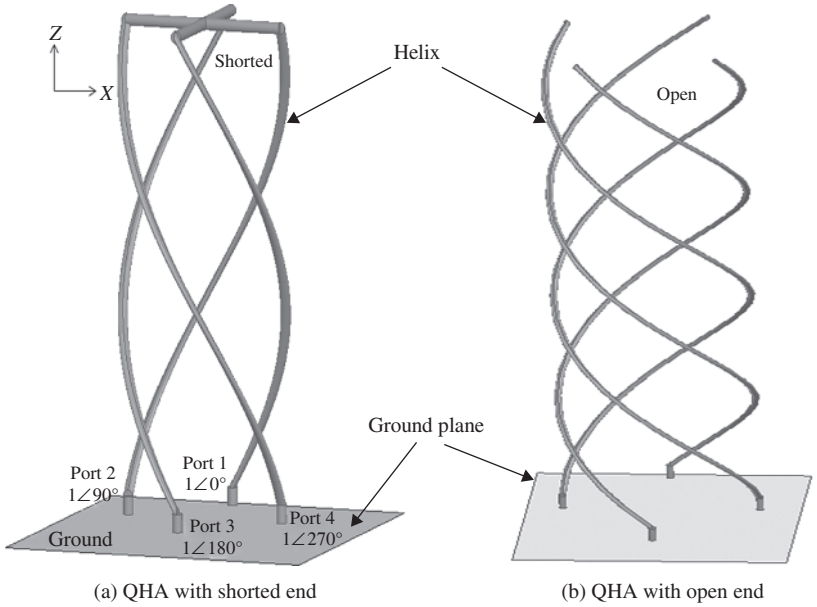

(a) QHA with shorted end (b) QHA with open end

Figure 1.14 Configurations of QHA

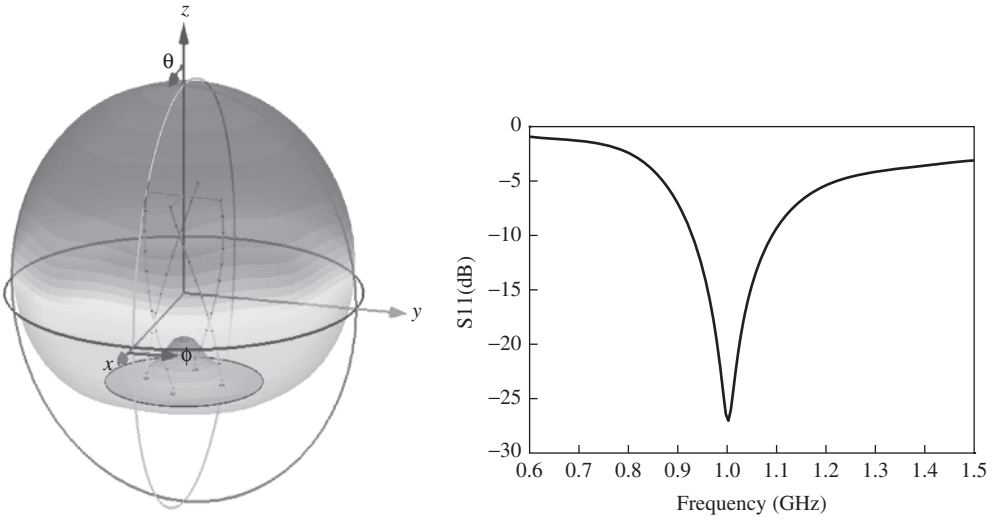

(a) Simulated radiation pattern of QHA (b) Simulated reflection coefficient

Figure 1.15 Simulated results of an end-shorted QHA

Here N is an integer number. When N is an even number, the helices should be shorted together, as shown in Figure 1.14(a); while when N is an odd number, the helices should be open-circuited, as shown in Figure 1.14(b).

Figure 1.15 shows the simulated results of an end-shorted QHA which has helices of $\lambda/2$ long and $^1/_2$ turn. Figure 1.15(a) shows the simulated radiation pattern of a QHA. As shown, QHA can achieve a wide-beam circularly polarized pattern, suitable for GPS signal reception. The simulated reflection coefficient results are shown in Figure 1.15(b). It is noted that, compared to the monofilar helical antenna, the QHA has a narrower bandwidth.

The QHA mentioned previously requires a separate phase quadrature network for providing 0^o, 90^o, 180^o and 270^o phases to each of four helices. Such a feed network increases the size and complexity of antennas. To alleviate this problem, self-phased QHA has been developed. In the self-phased approach, two bi-filars with different lengths are employed and the difference in lengths of bi-filars leads to a 90^o phase difference between them. As the self-phased QHA does not require a separate phase quadrature network, it reduces the size and complexity of QHA. QHA is a popular choice for handheld mobile terminals in mobile satellite communications due to its small size and hemi-spherical radiation patterns.

The fabrication of QHA will require accurate bending and shaping of wires which is not always easy. Figure 1.16 shows a PQHA, which is basically a printed version of QHA antennas. Four printed helices are wound around a cylinder as shown in Figure 1.16. The four printed helices are to be fed in phase quadrature in order to produce the desired hemispherical pattern. Compared to QHA antennas, PQHA is easier to fabricate in mass quantities and is lower cost, as the antennas can be fabricated using standard printed circuit board (PCB) technology. In addition, PQHA allows more flexibility in antenna designs. For example, it is easy to produce a PQHA with meandered-line helices patterns so as to reduce the antenna size [20]. Such a pattern will be, however, difficult to implement in wires

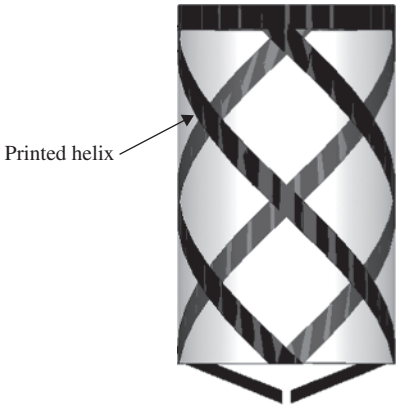

Figure 1.16 PQHA antenna

for QHA. The use of printed technology enables accurate fabrication of PQHA with less fabrication tolerance issues as in the case of QHA. Due to the use of PCB technology, it is also possible to integrate PQHA with microwave diodes or devices.

1.3.5 Spiral Antennas

Spiral antennas belong to the class of frequency independent antennas which operate over a wide range of frequencies. Radiation pattern, polarization and impedance of such antennas remain unchanged over a wide bandwidth [21]. Figure 1.17 shows one type of spiral antenna called an *Archimedean spiral antenna*. It includes two conductive arms, extending from the centre outwards. The antenna has a planar structure. Each arm of the Archimedean spiral is defined by the equation:

$$r = a\phi \tag{1.20}$$

Equation (1.20) states that the radius r of the antenna increases linearly with the angle ϕ. The parameter a is a constant which controls the rate at which the spiral flares out. Arm 2

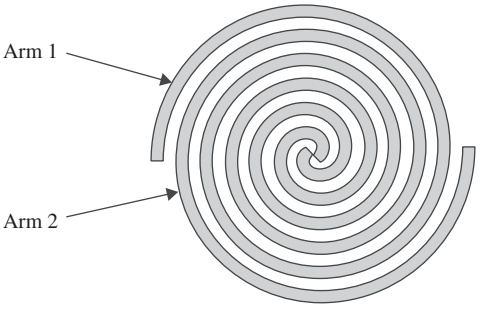

Figure 1.17 Spiral antenna

of the spiral is the same as the arm 1, but rotated at 180°. The direction of rotation of the spiral defines the direction of antenna polarization. Additional arms may be included to form a multi-spiral antenna. Usually the spiral is cavity backed, and the conductive cavity changes the antenna pattern to a unidirectional pattern. A two-arm spiral antenna shown in Figure 1.17 is excited in a balanced mode (that is, the same amplitude and a 180° phase difference between the two arms). Such a two-arm spiral radiates a CP wave in the antenna-axis direction normal to the antenna plane over a wide frequency range. For exciting this antenna, a coaxial line is used with a wideband balun circuit, which transforms the unbalanced mode of the coaxial line into the balanced mode required for the spiral antenna. It is noted that designing and installing such a wideband balun circuit for the spiral antenna requires considerable effort [21–23].

1.3.6 CP Dielectric Resonator Antennas

DRA is a resonant antenna fabricated from low-loss microwave dielectric materials. The resonant frequency of a DRA is a function of its size, shape and dielectric permittivity. Compared to other antenna types, DRA offers several attractive features. For example, DRA can achieve high radiation efficiency (>95%), flexible feed arrangement, simple structure, small size and the ability to produce different types of radiation patterns using different modes. In particular, DRA avoids conductor losses in patch antennas and is useful for applications at millimetre-wave frequencies. Various shapes of resonators can be used (rectangular, cylindrical, hemispherical, etc.), and various modes can be excited, producing broadside or conical-shaped radiation patterns for different coverage requirements. A wide range of permittivity values can be used (from about 6 to 100), thus antenna engineers can have control over the antenna size and bandwidth. A wideband DRA can be achieved using low permittivity while a compact size can be achieved with high permittivity.

Figure 1.18 shows a DRA antenna for circular polarization. A square DRA is fed by two orthogonal microstrip lines connected to a 90° microstrip hybrid. A metallic ground plane is at the bottom. This is a typical dual-feed technique as in the case of CP microstrip patch antennas. The required dual-feed network with a 90° microstrip hybrid takes up lots of space and increases the insertion loss (hence decreasing the radiation efficiency). An alternative

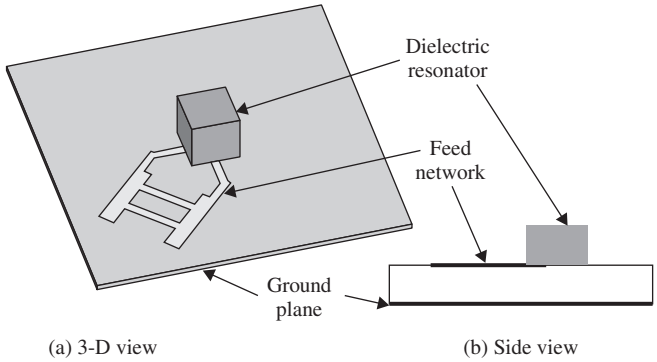

Figure 1.18 CP dielectric resonator antenna

technique is to employ a single-feed technique. As discussed in Section 1.3.1, a single-feed square patch antenna with perturbations can excite two orthogonal modes in the patch and achieve CP operation. Similarly, in the case of DRA, it can achieve CP by using a quasi-square DRA with a single feed. Compared to the single-feed microstrip patch antenna which usually achieves narrow CP bandwidth about 1–2% for 3dB AR, single-feed DRAs can achieve up to 7% CP bandwidth [24–26].

For a rectangular DRA, the resonant frequency can be calculated by

$$f_{MNK} = \frac{1}{2\sqrt{\varepsilon\mu}}\sqrt{\left(\frac{M}{l}\right)^2 + \left(\frac{N}{w}\right)^2 + \left(\frac{K}{h}\right)^2} \tag{1.21}$$

where ε is the permittivity,

μ is the permeability
M, N and K are integer numbers, and
l, w and h are the length, width and height of the rectangular DRA, respectively.

From equation (1.21), it can be seen that the DRA can resonate at various modes, and the resonant frequency is inversely proportional to the square root of the product of material parameters. A high permittivity material will lead to a low resonant frequency of DRA. DRA can be fed using different techniques such as probe feed, aperture slot coupling, microstrip lines and CPW.

1.3.7 CP Slot Antennas

The printed slot antenna is very simple in structure: it consists of a microstrip feed that couples electromagnetic waves through the slot above and the slot radiates them. A microstrip-fed slot antenna is flexible in integration with other active and passive devices in a hybrid microwave integrated circuit (MIC) and microwave monolithic integrated circuit (MMIC) design. They are also easy to make as they can be cut into the surface of the platform they are mounted on. Slot antennas are able to achieve a broader bandwidth compared to microstrip patch antennas. Figure 1.19 shows a CP printed slot antenna. As shown, a square slot is cut in the ground plane, and fed by a feed network at the bottom. The feed network uses a Wilkinson power divider in microstrip lines. The two branches of power divider have lengths with a difference of a quarter-wavelength, leading to a 90^o phase difference between two orthogonal modes in the slot excited by two orthogonal feed lines. Thus, circular polarization is produced in the square slot antenna.

To design a slot antenna, the length of slot is usually chosen to be a half-wavelength. The slot can take different shapes, such as a crossed slot, circular slot, annular ring, square ring and so on. Figure 1.20 shows another CP slot antenna which employs a circular slot fed by two orthogonal feed lines at the bottom. The printed slot antenna is easy to fabricate, has a low profile and low cost. However, the use of dual feeds and a feed network at the bottom as shown in Figures 1.19 and 1.20 occupies lots of space below the ground plane. For some applications, it is necessary to simplify the feed network by using a single feed instead. Figure 1.21 shows an example, which is basically a printed square slot antenna fed by a single microstrip line at the bottom. To achieve circular polarization, an L-shaped

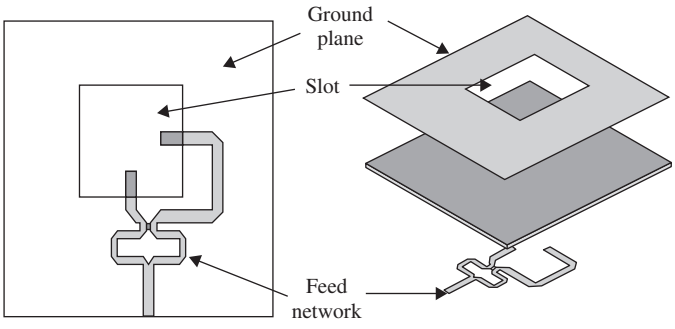

(a) Top view (b) 3-D view

Figure 1.19 CP square slot antenna fed by a microstrip network at bottom

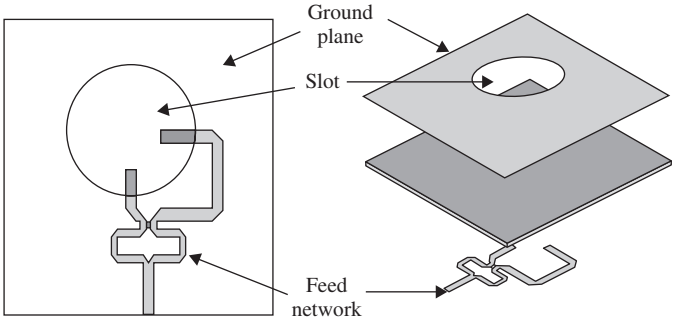

(a) Top view (b) 3-D view

Figure 1.20 CP circular slot antenna fed by a microstrip network

microstrip line is employed and the line excites two orthogonal modes in the square ring slot. The L-shaped microstrip line has a length of a quarter-wavelength, thus a 90° phase difference between two orthogonal modes in the slot is achieved. Such a CP slot antenna has a very simple feed network and is easy to implement.

In addition to the microstrip line feed shown previously, slot antennas can also be excited using other techniques such as coaxial cable or CPW. One drawback of these CP slot antenna is bi-directional radiation, as the slot will also radiate in the backward direction. Another ground plane can be added at the bottom so that the antenna can achieve broadside radiation only.

1.3.8 CP Horn Antennas

Horn antennas belong to the aperture antenna category, and their radiation performance is determined by the field distribution over the horn aperture. Horns are designed to provide a smooth transition between the feed waveguide and a wide aperture which serves to focus the main beam. Horns have found wide applications in satellite communications either as

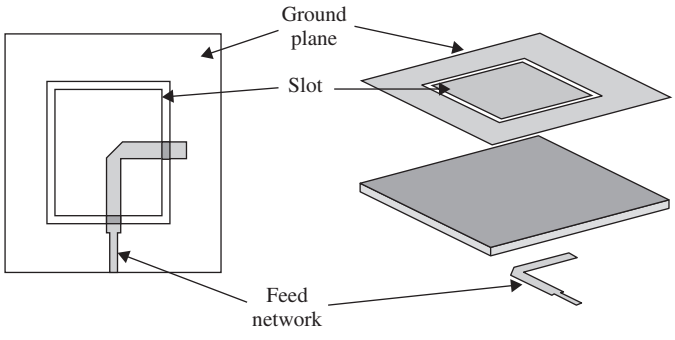

Figure 1.21 CP ring slot antenna fed by an L-shaped feed

earth coverage antennas or feeds for reflector antennas. Theory and design of horn antennas with linear polarization are well documented in [7–9,11,27].

Most of the horn antennas reported have a single feed and can radiate linear polarization radio waves [27]. CP horn antennas can be realized by using a horn with dual orthogonal feeds and a 90° hybrid. However, the performance of dual linear polarized horn antennas, such as the ridged horn antenna, suffers from manufacturing and assembling tolerances. Also, the use of a 90° hybrid adds more complexity and losses in antennas. During recent years, many new techniques of CP horn antennas have been proposed [28,29]. A typical configuration of CP horn antennas includes three major elements, that is, a wave launcher, a polarizer and a beam shaper, as shown in Figure 1.22 [28,29].

The wave launcher in Figure 1.22 consists of two probes at input ports 1 and 2, which can achieve RHCP and LHCP, respectively. The input probes are located nearly one quarter-wavelength from the short-circuited end of the waveguide section 1, as shown in the figure. Waveguide 1 is a circular waveguide which allows the propagation of waves in TE11 mode [27–29].

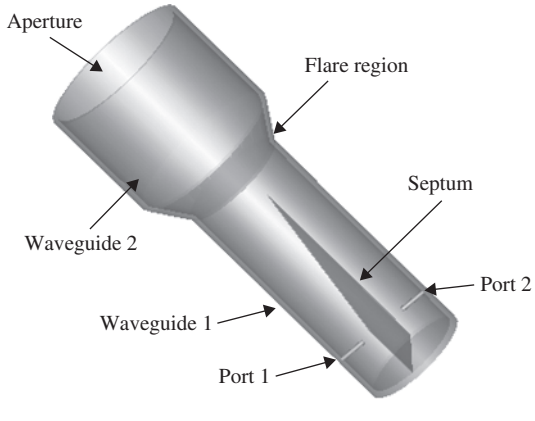

Figure 1.22 Configuration of a CP horn antenna

The polarizer in Figure 1.22 consists of a circular waveguide divided into two identical semi-circular waveguides by a septum. The septum can use either a dielectric septum or a metallic septum. A metallic septum with sloped height is shown in Figure 1.22. In some cases, a metallic septum with stepped height can be employed to achieve a broadband performance [28,29]. By selecting the appropriate dimensions of the septum's steps, the TE11 excitation converts into two orthogonal TE11 modes of equal amplitude and 90° out of phase. The dimensions of the septum steps are very critical if these two conditions are to be met simultaneously over a wide frequency range. In the case that two excitation ports are used for obtaining RHCP and LHCP waves, high isolation between two ports is required.

The beam shaper in Figure 1.22 is a dual-mode circular waveguide (denoted as waveguide 2 in the Figure) which allows the propagation of waves in both TE11 and TM11 modes. Note that waveguide 2 has a larger diameter than that of the circular waveguide section 1, and there is a flare region between the two waveguides. The length of waveguide 2 is chosen such that the TE11 and TM11 modes' relative phase and amplitude allow the cancellation of the electric field at the aperture boundary, which results in a reduction of undesired sidelobes. A CP horn using a sloped septum can achieve about 10% 3-dB AR bandwidth and 40 dB isolation between two ports, while the use of a stepped septum can increase the bandwidth to 25% at the expense of lower isolation (about 20∼25 dB) between two ports.

Other CP horn antennas have also been reported. For example, a horn excited with an L-shaped probe can be used to generate CP with 3 dB AR bandwidth of about 20% [30]. In [31], an oval shape waveguide polarizer is fed into a pyramidal horn antenna and a 3-dB AR bandwidth of 18% is reported. Note that the cross-section dimensions of the polarizer and horn antenna at the transition are different and they must be impedance-matched to minimize the generation of higher order modes.

1.3.9 CP Arrays

Previous sections have introduced different types of CP antenna elements. An array antenna consists of a number of antenna elements whose radiation is combined together to provide highly directive patterns. CP array antennas are needed in many applications such as satellite communications, inter-satellite communications, transmitting antennas onboard GPS satellites, and so on [11].

The array can have different configurations such as a 1D linear array or a 2D planar array. Figure 1.23 shows a 2D planar CP array with nine identical antenna elements. As shown, each element is a CP antenna with a square patch fed by two probe feeds located at two orthogonal edges of the patch with a 90° phase difference between them. Other types of antenna elements such as helix, DRA and so on, can also be employed to form CP arrays.

Assuming identical elements are employed and regular geometries are adopted in an array, the radiation pattern of the array can be obtained from the multiplication of radiation pattern of a single element, $E_{element}(\theta, \varphi)$, and the array factor $AF(\theta, \varphi)$ [7]:

$$E(\theta, \varphi) = E_{element}(\theta, \varphi) AF(\theta, \varphi) \tag{1.22}$$

The array factor is a function of the array geometry, the inter-element distance, the element excitation in amplitude and phase, the number of elements and the frequency. For a 1D linear array of N identical elements which are equally spaced along the z-axis and excited with the

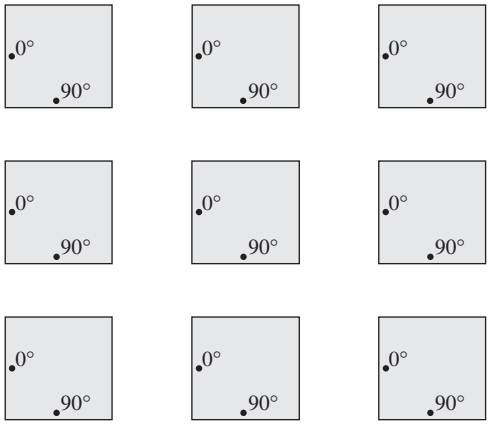

Figure 1.23 A nine-element CP array

same amplitude and phase, the array factor is

$$AF(\theta, \varphi) = \frac{\sin\left(\frac{N\psi}{2}\right)}{\sin\left(\frac{\psi}{2}\right)} \tag{1.23}$$

where $\psi = kd\cos\theta + \beta$ and $k = \frac{2\pi}{\lambda}$. Note a spherical coordinate system is employed. d and β denote the distance between elements and the phase shift between successive elements, respectively. For fixed-beam CP arrays, β is set to be a fixed value. The main beam of the CP array can be moved dynamically to point in different directions by changing β electronically. This is called a *phased array* [6,7,11,12]. Design techniques for CP arrays will be discussed in Chapter 5.

1.4 Antenna Modelling Techniques

1.4.1 Analytical Methods

Lots of analytical methods have been developed to analyse CP microstrip antennas, wire antennas, helical antennas, slots and DRA. For example, transmission-line models and cavity models have been developed for analysis and modelling of microstrip antennas [6–9,12,13]. Analytical methods have also been employed in the analysis of CP arrays [32,33]. These methods are very useful as they can provide a good insight into the physical mechanism of antenna operations. The drawback is the lack of accuracy, as these methods are usually based on some approximate assumptions.

1.4.2 Full-Wave Methods

The rapid development of computer technology has driven the development of various numerical methods during the past few decades. Full-wave methods mainly include the method of moments (MOM), the finite element method (FEM), and the finite difference

time-domain (FDTD) method. These methods are accurate as they directly solve Maxwell's equations without making physical approximations [34]. The precision of these methods is mainly dependent on the mesh discretization.

MOM is a versatile numerical method for solving integral equations [35]. One advantage of MOM is the variational nature of its solution: even if the unknown field is modelled to first order accuracy, the solution of MOM is accurate to the second order. MOM involves a significant amount of pre-processing of Maxwell's equations because it needs to use Green's function. MOM has been widely applied in analysis and modelling of all types of CP antenna elements and arrays. One disadvantage of MOM is that it needs to find the Green's function for a specific problem which can be difficult in some cases.

FEM is a numerical method for solving boundary value problems characterized by a partial differential equation and a set of boundary conditions [36]. The main advantage of FEM is that only a very sparse linear system is required to be solved, thus the memory requirement scales linearly with the number of degrees of freedom. In addition, the natural treatment of complex media makes FEM a very popular and powerful method in dealing with inhomogeneous structures. One disadvantage of FEM is the difficulty in dealing with open problems such as antennas. For antennas analysis and modelling, artificial absorbing boundary conditions (ABC)s, such as perfectly matched layers, should be applied around the object to simulate the radiation condition [37–41]. This increases the complexity and instability, unfortunately.

The FDTD method is another popular differential equation-based computational algorithm for antennas modelling [42,43]. Basically it is a time-domain numerical solver. It is simple to program, highly efficient and can be easily adopted. Also it can provide information of antenna radiation in the time domain, which is very useful in many cases such as wideband CP antennas. Fourier transforms are performed to obtain frequency-domain information if needed. Compared to FEM and MOM, the FDTD method can deal with large-scale array antennas simulation by using the parallel computation [44]. Furthermore, it is also a matrix-free technique. In recent years, the application of conformal meshes enables the FDTD method to analyse 3D antennas with curved structures [45,46].

1.5 Typical Requirements and Challenges in CP Antenna Designs

The requirements for CP antennas depend on the specific application: During recent years there has been an increasing demand for high data-rate broadband communication links using Ka-band mobile satellite communication systems [47]. The antenna can be put on board airplanes (e.g. for Internet in the sky), high-speed trains or cars. Such applications require CP antennas which have high gain, low profile, low mass, can be easily fabricated and are able to scan the beam electronically within a wide angle range in order to guarantee the service availability to the coverage areas. Future millimetre-wave WLAN and GNSS remote sensing will also require ultra-compact light-weight, low cost, wideband/multi-band high gain CP antennas with fast beam-scanning capability and low cost [48]. For mobile terminals in mobile communications or satellite communications, it is desirable to have small-size smart antennas at low cost [49].

GNSS receivers will need to be more compact, receive more signals and obtain higher accuracy in positioning, thus requiring miniaturized multi-band CP antennas which can cover all frequency bands of GNSS (GPS, Galileo, GLONASS, Compass, etc.), are low

cost, stable phase centres, the capability of multipath mitigation and adaptive patterns (for anti-jamming purposes) and are easy to integrate with RF circuits (filters, low noise amplifiers, mixers, etc.) [50–52].

RFID applications will require miniaturization of CP antennas with broadband, high gain, low cost and high reliability [53–55]. Future multi-band multi-function mobile terminals will require wideband/multi-band/multi-mode antennas which are re-configurable and can cover a variety of services such as (global system for mobile communications (GSM), Universal mobile telecommunications system (UMTS), mobile satellite communications, WLAN, GNSS, RFID, digital video broadcasting-handheld, etc.) while being small and low cost. The application of multiple inputs and multiple outputs (MIMO) technique into land mobile satellite communication will require broadband dual CP antennas. The growing of fields such as Internet of Things (IOT) [56,57], Long Term Evolution (LTE) [58], Cognitive Radio [59,60], body-centric wireless networks [61], satellite communication advanced flexible telecom payloads [11,47], small satellites (micro-sat, nano-sat, cube-sat) and formation flying [62–64], wireless power transmission, millimetre-wave, sub-millimetre-wave and terahertz systems [65] will drive the need for more innovative high-performance CP antennas.

The requirements here lead to lots of interesting challenges for antenna engineers. Typical challenges include the miniaturization of CP antennas, multi-band CP antennas, wideband CP antennas, high gain CP antennas, reconfigurable CP antennas, electronically beam steering CP antennas and so on. Chapters 2–5 will discuss various techniques of advanced CP antenna designs to meet these requirements. Some case studies will be provided in Chapter 6.

1.6 Summary

This chapter introduces basic parameters of antennas such as input impedance, reflection coefficient, gain, directivity, radiation pattern and antenna polarization. Different types of CP antennas including microstrip patch CP antennas, crossed dipoles, helix antennas, QHA, PQHA, spiral antenna, DRA, slot antenna, CP horns and CP arrays are also discussed. Basic principles of the operation of each antenna type are explained. Typical requirements and challenges of CP antenna designs are also discussed. Besides the CP antenna types mentioned, there are many other types of CP antennas, which can be realized using waveguide antenna, reflectors, lens antenna, leaky-wave antennas, slot arrays, hybrid combinations of different antennas, and so on [6–13].

References

[1] Braasch, M.S., Multipath effects, in *Global Positioning System: Theory and Applications*, Edited by Parkinson, B.W. et al., American Institute of Aeronautics and Astronautics (AIAA), 1, pp. 547–568, 1996.
[2] Counselman, C.C., Multipath rejecting GPS antennas, *Proceedings of IEEE*, 87(1), pp. 86–91, January 1999.
[3] Davies, K., *Ionospheric Radio Propagation,* NBS Monograph 80, 181, US Government Printing Office, Washington, DC, 1965.
[4] Brookner, E., W.M. Hall, and R.H. Westlake. Faraday loss for L-band radar and communications systems. *IEEE Transactions on Aerospace and Electronic Systems*, 21(4): 459–469, 1985.
[5] Pozar, D.M., *Microwave Engineering*, 2nd edn, John Wiley & Sons, Inc., 1997.
[6] Nakano, H. *Helical and Spiral Antennas: A Numerical Approach*, Research Studies Press Ltd, 1987.
[7] Balanis, C.A. *Antenna Theory: Analysis and Design*, Hoboken, NJ: John Wiley & Sons, Inc., 2005.

[8] Stutzman, W.L. and G.A. Thiele. *Antenna Theory and Design*, 2nd edn, New York: John Wiley & Sons, Inc., 1997.
[9] Kraus, J.D. and R.J. Marhefka. *Antennas for all Applications*, New York: McGraw-Hill, 2002.
[10] Toh, B.Y., R. Cahill and V.F. Fusco. Understanding and measuring circular polarisation, *IEEE Trans. Education*, 46: 313–318, 2003.
[11] Imbraile, W., S. Gao and L. Boccia. (eds), *Space Antenna Handbook*, Chichester: John Wiley & Sons, Ltd, 2012.
[12] Pozar, D.M. and D. Schaubert (eds). *Microstrip Antennas: The Analysis and Design of Microstrip Antennas and Arrays*, New York: John Wiley & Sons, Inc., 1995.
[13] James, J.R. and P.S. Hall (eds.). *Handbook of Microstrip Antennas*, IEE Electromagnetic Waves Series, 1989.
[14] Hirota, T., A. Minakawa and M. Muraguchi. Reduced-size branch-line and rat-race hybrids for uniplanar MMICs, *IEEE Trans. Microw. Theory Tech.*, 38(3): 270–275, Mar.1990.
[15] Okabe, H., C. Caloz and T. Itoh. A compact enhanced-bandwidth hybrid ring using an artificial lumped-element left-handed transmission-line section, *IEEE Trans. Microw. Theory Tech.*, 52(3): 798–804, Mar. 2004.
[16] King, H.E., J.L. Wong and E.H. Newman. *Antenna Engineering Handbook*, Chapter 12. McGraw-Hill, 2007
[17] Kilgus, C.C. Resonant quadrifilar helix, *IEEE Trans. Antenna and Propagation*, vol. AP-17, 349–451. May 1969.
[18] Best, S.R. A 7-turn multi-step quadrifilar helix antenna providing high phase center stability and low angle multipath rejection for GPS applications, *IEEE Antennas and Propagation Society International Symposium*, Vol. 3, pp. 2899–2902, 2004.
[19] Tranquilla, J.M. and S.R. Best. A study of the quadrifilar helix antenna for Global Positioning System (GPS) applications', *IEEE Transactions on Antennas and Propagation*, 38: 1545–1550, 1990.
[20] Bandari, B., S. Gao and T. Brown. Compact printed quadrifilar helix antennas with broadband performance, in *Proc. Loughborough Antennas and Propagation Conference*, UK, pp. 325–328, Nov. 16–17, 2009.
[21] Nakano, H., K. Nogami, S. Arai, , H. Mimaki and J. Yamauchi. A spiral antenna backed by a conducting plane reflector, *IEEE Transactions on Antennas and Propagation*, 34(6): 791–796, June 1986.
[22] Bawer, R. and J. Wolfe A printed circuit balun for use with spiral antennas', *IEEE Transactions on MTT*, 8(3): 319–325, May 1960.
[23] Tu, W.H. and K. Chang. Wide-band microstrip to-coplanar stripline/slotline transitions, *IEEE Transactions on MTT*, 54(3): 1084–1089, March 2006.
[24] Leung, K.W. and H.K. Ng. Theory and experiment of circularly polarized dielectric resonator antenna with a parasitic patch, *IEEE Trans. Antennas Propag.*, 51: 405–412, Mar. 2003.
[25] Oliver, M.B., Y.M. Antar, R.K. Mongia and A. Ittipiboon. Circularly polarized rectangular dielectric resonator antenna, *Electron. Lett.*, 31: 418–419, Mar. 1995.
[26] Chair, R., S. Yang, A.A. Kishk, K.F. Lee and K.M. Luk. Aperture fed wideband circularly polarized rectangular stair shaped dielectric resonator antenna, *IEEE Trans. Antennas Propag*., 54(4): 1350–1352, 2006.
[27] Olver, A.D., P.J.B. Clarricoats, A.A. Kishk and L. Shafai. *Microwave Horns and Feeds*, London, New York: IEEE Press, 1994.
[28] Hazdra, P., R. Galuscak and M. Mazanek. Optimization of prime-focus circular waveguide feed with septum polarization transformer for 1 .296 GHz EME station, *Proceedings of the First European Conference on Antennas and Propagation (EuCAP)*, Nice, France, November 2006.
[29] Franco, M.J. A high-performance dual-mode feed horn for parabolic reflectors with a stepped septum polarizer in a circular waveguide', *IEEE Antennas and Propagation Magazine*, 53(3): 142–146, June 2011.
[30] Fukusako, T. and L. Shafai. Design of broadband circularly polarized horn antenna using an L-shaped probe, *Proceedings of IEEE Antennas and Propagation Society International Symposium 2006*, pp. 3161–3164, July 2006.
[31] Jung, Y.B. Ka-band polarizer structure and its antenna application, *Electronics Lett.*, 45(18): 1379–1381, Aug. 2009.
[32] Hall, P.S and J.S. Dahele. Dual and circularly polarised microstrip antennas, invited chapter in Lee, K.F. and Chen, W. (eds), *Advances in Microstrip and Printed Antennas'*, New York: John Wiley & Sons, Inc., pp. 163–217, 1997.
[33] Hall, P.S., J.S. Dahele and J.R. James. Design principles of sequentially fed wide bandwidth circularly polarised microstrip antennas, *IEE Proc.*, pt H, 136(5): 381–389, Oct 1989.
[34] Peterson, A.F., S.L. Ray and R. Mittra. *Computational Methods for Electromagnetics*, The IEEE/OUP Series on Electromagnetic Wave Theory and Oxford University Press, 1997.

[35] Rao, S.M., D.R. Wilton and A.W. Glisson. Electromagnetic scattering by surfaces of arbitrary shape, *IEEE Transactions on Antennas and Propagation*, 30(3): 409–418, 1982.
[36] Alett, P.L., A.K. Baharani and O.C. Zienkiewicz. Application of finite elements to the solution of Helmholtz's equation, *IEE Proceedings*, 115: 1762–1766, 1968.
[37] Sacks, Z.J., D.M. Kingsland, R. Lee, et al. A perfectly matched anisotropic absorber for use as an absorbing boundary condition', *IEEE Transactions on Antennas and Propagation*, 43(12): 1460–1463, 1995.
[38] Berenger, J.P. A perfectly matched layer for the absorption of electromagnetic waves, *Journal of Computational Physics*, 114: 185–200, 1994.
[39] Silvester, P.P. and R.L. Ferrari. *Finite Elements for Electrical Engineers*, 2nd edn, Cambridge: Cambridge University Press, 1990.
[40] Jin, J.M. *The Finite Element Method in Electromagnetics*, New York: John Wiley & Sons, Inc., 1993.
[41] Volakis, J.L., C. Arindam and L.C. Kempel. *Finite Element Method for Electromagnetics: Antennas, Microwave Circuits, and Scattering Applications*, New York: Wiley-IEEE, 1998.
[42] Kunz, K.S. and R.J. Luebbers. *The Finite Difference Time-domain Method for Electromagnetics*, Boca Raton, FL: CRC Press, 1993.
[43] Taflove, A., *Computational Electrodynamics: The Finite-Difference Time-Domain Method*, Norwood, MA: Artech House, 1995.
[44] Yu, W., R. Mittra, T. Su, Y. Liu and X. Yang. *Parallel Finite-Difference Time-Domain Method*, Artech House Publisher, July 2006.
[45] Dey, S. and R. Mittra. A locally conformal finite-difference time-domain (FDTD) algorithm for modeling three-dimensional perfectly conducting objects, *IEEE Microwave and Guided Wave Letters*, 7(9): 273–275, 1997.
[46] Yu, W. and R. Mittra. *CFDTD: Conformal Finite-Difference Time-Domain Maxwell's Equations Solver, Software and User's Guide*, Artech House Publisher, 2004.
[47] Evans, B. *Satellite Communication Systems*, 3rd edn, IET Publisher, 1999.
[48] Unwin, M., S. Gao, R. Steenwijk, P. Jales, M. Maqsood, C. Gommenginger, et al. Development of low-cost spaceborne multi-frequency GNSS receiver for navigation and GNSS remote sensing, *International Journal of Space Science and Engineering*, 1(1): 20–50, Jan. 2013. *(invited paper)*
[49] Liu, H., S. Gao and T. Loh. Electrically small and low cost smart antenna for wireless communication, *IEEE Trans. on Antennas and Propagation*, 60(3): 1540–1549, March 2012.
[50] Öhgren, M., M. Bonnedal and P. Ingvarson, Small and lightweight GNSS antenna for previse orbit determination, *Proc. of 2010 ESA Space Antennas Workshop*, Noordwijk, Netherlands, Section 16, pp. 1–5, Oct. 2010.
[51] Chen, C.C., S. Gao and M. Maqsood. Antennas for Global Navigation Satellite Systems receivers, Chapter 14 in *Space Antenna Handbook*, Imbriale, W., Gao S. and Boccia L. (eds), Chichester: John Wiley & Sons, Ltd, 2012.
[52] Chen, X., C. Parini, B. Collins, Y. Yao and M. Rehman. Antennas for global navigation satellite systems, Hoboken, NJ: John Wiley & Sons, Inc., 2012.
[53] Chen, Z.N. (ed.) *Antennas for Portable Devices*, Chichester: John Wiley & Sons, Ltd, March 2007.
[54] Nasimuddin, X. Qing, and Z.N. Chen. Compact circularly polarized symmetric-slit microstrip antennas, *IEEE Trans. Antennas Propagat.*, 59(1): 285–288, Jan. 2011.
[55] Wong, K.L. *Planar Antennas for Wireless Communications*, New. York: John Wiley & Sons, Inc., 2003
[56] Ashton, K. That 'Internet of Things' thing, *RFID Journal*, 22 July. 2009, [Internet] Available at: www.rfidjournal.com/article/view/4986 [Accessed 13 August 2013].
[57] EPoSS. *The Internet of Things – EpoSS*, 2011 [Internet] Available at: www.smart-systems-integration.org/public/news-events/events/internet-of-things-week-2011. [Accessed 13 August 2013].
[58] Ghosh, A., R. Ratasuk, B. Mondal, N. Mangalvedhe, and T. Thomas. LTE-advanced: next-generation wireless broadband technology, *IEEE Wireless Communications*, 17(3): 10–22, June 2010.
[59] Wang, J., M. Ghosh and K. Challapali. Emerging cognitive radio applications: a survey, *IEEE Communications Magazine*, 49(3): 74–81, 2011.
[60] Nguyen, V., F. Villain and Y. Guillou. *Cognitive Radio RF: overview and challenges*, *VLSI Design*, Hindawi Publishing Corporation, 1–13, 2012.
[61] Patel, M. and J. Wang, Applications, challenges, and prospective in emerging body area networking technologies, *IEEE Wireless Communications Magazine*, 17(1): 80–88, 2010.
[62] Gao, S., K. Clark, M. Unwin, J. Zackrisson, W.A. Shiroma, J. Akagi, et al. Antennas for modern small satellites, *IEEE Antennas and Propagation Magazine*, 51(4):40–56, Dec. 2009.

[63] Gao, S., K. Clark, J. Zackrisson, K. Maynard, L. Boccia and J.D. Xu. Antennas for Low-Cost Small Satellites, Chapter 15 in *Space Antenna Handbook*, Imbriale, W., Gao, S. and Boccia, L. (eds), Chichester, John Wiley & Sons, Ltd, 2012.

[64] Barnhart, D., T. Vladimirova and M.N. Sweeting. Very small satellite design for distributed space missions, *Journal of Spacecraft and Rockets*, 44(6): 1294–1299, Dec. 2007.

[65] Hebling, J., K.L. Yeh, M. Hoffmann, B. Bartal and K. Nelson. Generation of high power terahertz pulses by tilted-pulse-front excitation and their application possibilities, *Journal of Opt. Soc. Am. B*, 25: B6, 2008.